

Static and Ultrafast Optical Response of Two Ag Nanospheres Glued by a CdTe Quantum Dot.

Sabina Gurung^{1,2}, Asha Singh¹, Durga Prasad Khatua^{1,2},
Himanshu Srivastava³, and J. Jayabalan^{1,2,*}

¹Nano Science Laboratory, Materials Science Section, Raja Ramanna Centre for Advanced Technology, Indore, India - 452013.

²Homi Bhabha National Institute, Training School Complex, Anushakti Nagar, Mumbai, India - 400094.

³Lithography and Microscopy Laboratory, Synchrotrons Utilization Section, Raja Ramanna Centre for Advanced Technology, Indore, India - 452013.

E-mail: *jjaya@rrcat.gov.in

Abstract. A hot-spot of high local field can be created in between two closely placed metal nanoparticles by irradiating them with an appropriate wavelength and polarization of incident light. The strength of the field at the hot-spot is expected to get enhanced by even up to six orders of magnitude than that of the applied field. Placing a semiconductor quantum dot or an analyte molecule at the hot-spot is an essential step towards harnessing the enhanced field for applications. In this article, we show that it is possible to position a CdTe quantum dot (QD) between two larger silver nanospheres in colloidal solution. The extinction spectra measured during growth suggests that the final hybrid nanostructure have two touching Ag nanoparticles (NPs) and a CdTe QD in between them close to the point of contact. Using ultrafast transient measurements, it has been shown that the presence of CdTe QD strongly influence the dynamics when the probe excites the hot-spot. The method demonstrated here to place the semiconductor QD in between the two Ag NPs is an important step in the area of colloidal self-assembly and for application of hot-spot in plasmonic sensing,

optoelectronics, energy-harvesting, nanolithography, and optical nano-antennas.

1. Introduction

When excited at localized surface plasmon resonance (LSPR) the metal nanoparticle (NP) can significantly enhance the strength of electromagnetic field around them [1, 2]. Such field enhancement can be as large as 20 times than that of the applied [3]. This property of metal NP opened up its applications in plasmonic sensing, optoelectronics, energy harvesting, nanolithography, nano-antennas and imaging [4–12]. A second generation of local field enhancement is realized when two metal NPs are placed close to each other with separation less than few nanometers. The field in between these particles can be enhanced by a factor of up to six orders of magnitude than that of the applied. Theoretical studies on generation of such high field regime, known as the hot-spot, using two metal nanoparticles of various size, shape and orientation is being studied by various groups [13, 14]. In past, bottom up techniques such as chemical synthesis was used for the preparation of large quantity of isolated metal nanoparticles of different shapes with good size and crystal quality [15–17]. To generate hot-spots, these particles were simply aggregated in the colloid. Such random hot-spots in aggregates were also used for increasing the SERS signals from molecules [16]. Recently dimer shaped Ag nanoparticles, which can show hot-spot, was prepared in colloidal form by controlled addition of linking polymer or salt to Ag nanosphere colloid. When mixed, the linker molecule acts as glue to stick the two larger sized metal NPs. Because this glue is tiny, further attachment of metal NP to the same spot is prevented, creating the desired dimer structure [18, 19]. There are other similar solution based techniques to prepare dimers [20, 21]. All these dimer preparation methods require high level of control over the number of linking molecules verses the number of nanoparticles to avoid

formation of large aggregates. Although such techniques allow preparation of hot-spot, placing a semiconductor QD or an analyte molecule in that location is also important for harnessing the enhanced local field for applications. Once placed at the hot-spot, the material will experience a strong field leading to enhancement in its absorption, emission and pronounced Fano-like effect and so forth [22, 23].

In this article, we show that by mixing Ag NP colloid with TGA capped CdTe QDs in a particular mixing ratio, it is possible to prepare hybrid nanostructure with CdTe QD stuck in between two Ag NPs. By comparing the measured time evolution of extinction spectra during self-organized growth of the hybrid nanostructure with that of the calculated, we explain the process of hybrid formation. Ultrafast pump-probe measurements can provide quantitative information regarding complex processes that take place between the metal and semiconductor nanocomposites. Using ultrafast transient transmission measurements it has been shown that the carrier dynamics in the hybrid colloid is effected only when probed by a light that generates high field in between Ag NPs. The method demonstrated here to place the semiconductor QD in between the two Ag NPs is an important step in the area of colloidal self-assembly and for application of hot-spot in plasmonic sensing, optoelectronics, energy -harvesting, nanolithography and optical nano-antennas.

2. Experimental Details

The individual constituents of the hybrid nanostructure, citrate capped silver NPs and TGA capped CdTe QDs dispersed in water, were prepared separately by wet chemical methods [24–26]. The procedure followed for the preparation of this individual colloids has been reported earlier [27]. Ag-CdTe hybrid colloid, labeled H_γ , is prepared by mixing V_p , volume of Ag NP colloid and V_d , volume of CdTe QD colloid. Here the mixing ratio,

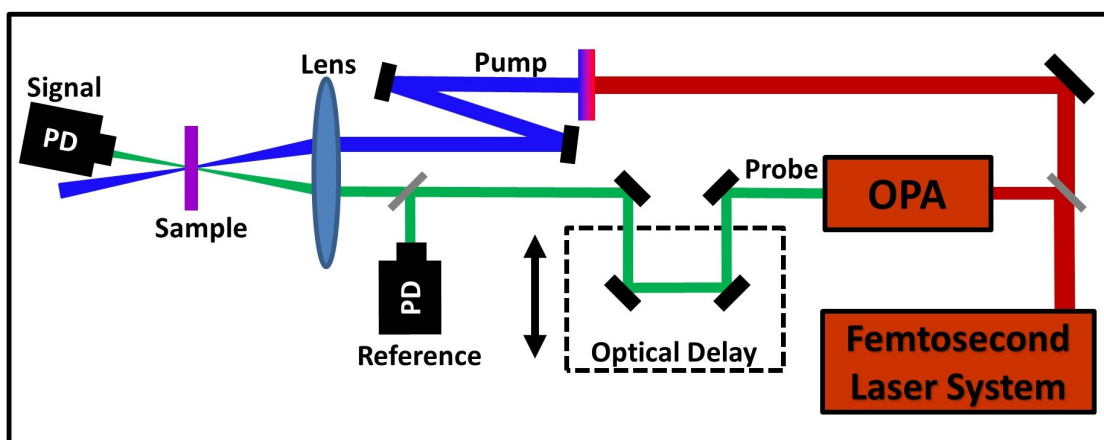


Figure 1: Schematic of the pump-probe setup used for the measurement of transient transmission from the samples.

γ , is defined as V_p/V_d . In the mixed solution the Ag-CdTe hybrid nanostructures are expected to form because of self-organized growth [17,27–29]. A 1 kHz, 35 femtosecond oscillator-amplifier system was used for the transient transmission measurements in standard pump-probe geometry (Fig.1). The pump beam (400 nm) for the experiment was obtained by generating second harmonic of a part of the 800 nm beam from the laser system using a BBO crystal. The 800 nm beam was also used for pumping an optical parametric amplifier (OPA). A fraction of the OPA output beam (408 nm or 550 nm) was used for probing the optical response of the sample. The polarization of the 408 nm and 550 nm beams were parallel and perpendicular to that of pump beam respectively. The sample was constantly circulated in a 1 mm cell to avoid any thermal damage.

3. Results and Discussion

Figure.2a shows the extinction spectrum of the Ag NP colloid and CdTe QD colloid. The extinction spectrum of the Ag NP colloid shows a single peak at 413 nm which corresponds to the LSPR of small silver nanospheres dispersed in water [30,31]. The

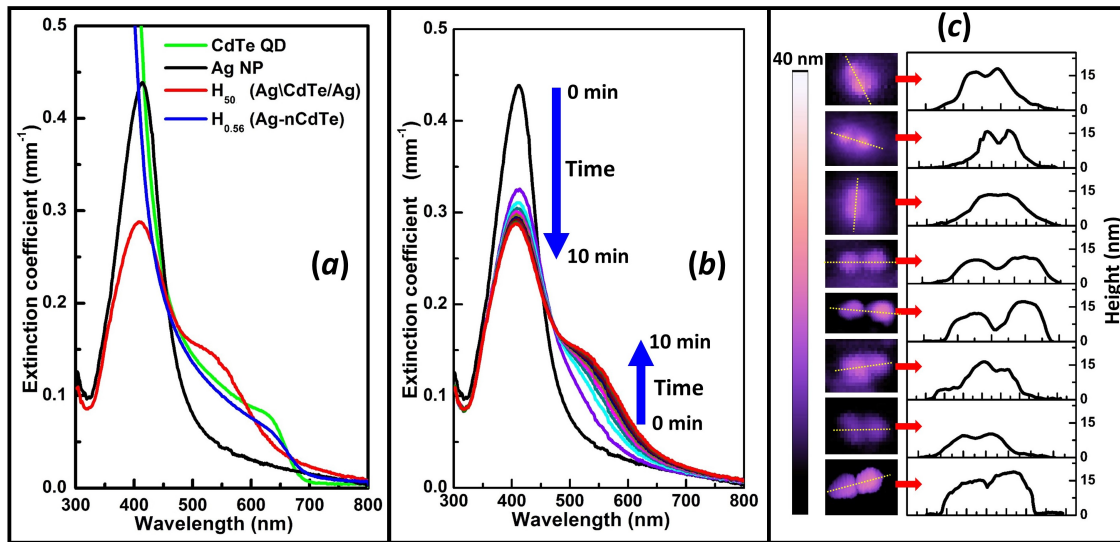


Figure 2: Static optical and structural characterization of individual, mixed and hybrid colloids: (a) Extinction coefficient of CdTe QD, Ag NP, H₅₀ hybrid and H_{0.56} hybrid colloids. (b) The time evolution of extinction spectrum of the mixed colloid from just after mixing to about 10 min. (c) Representative AFM images of hybrid nanostructures present in the H₅₀ hybrid colloid. x is the distance along the substrate surface.

extinction spectrum of the CdTe QD colloid shows exciton peak at 635 nm which is due to 1s(e)-1s(h) transition [32–34]. For structural characterization few drops of these samples were dried on a mica substrate and the topography of the surface was measured using Atomic Force Microscope (AFM). Some representative AFM images of the individual colloids are shown in Fig.S1 of supporting information (SI). The image that corresponds to individual Ag NP colloid and CdTe QD colloid shows presence of mostly well separated particles. The average diameter of the Ag nanoparticles and CdTe QDs measured using the height profile from these AFM images are 17 nm and 3.5 nm respectively.

Ag-CdTe hybrid sample, H₅₀ was prepared by mixing CdTe QD colloid with Ag NP colloid at a mixing ratio of $\gamma = 50$. Immediately after the addition, the LSPR peak red-shifts slightly and at the same time the extinction peak height reduces to about 74% of that before addition (Fig.2b). Although the red-shift is very small, repeated preparation

shows that the red-shift do occur at about 1 min after mixing (Fig.S2). Over the period of next few minutes another peak appears on the red-side. For example, the spectrum of the sample taken after 2 min could be fit well with two Gaussian peaks (Fig.3a). From 2 min to 10 min, the original LSPR peak blue-shifts and continues to reduce in strength. Whereas the longer wavelength peak red-shifts and grows (Fig.2b). After about 10 minutes, the mixed colloid shows no further change in the spectrum. The final stable hybrid sample thus formed (H_{50}) has peaks at 410 nm and 535 nm with strength 65% and 32% compared to that of bare Ag NP colloid respectively. Note that, the sample would be continuously evolving during the measurement of the spectra. Nevertheless, the measured spectra can be used for gaining insight into the hybrid formation process.

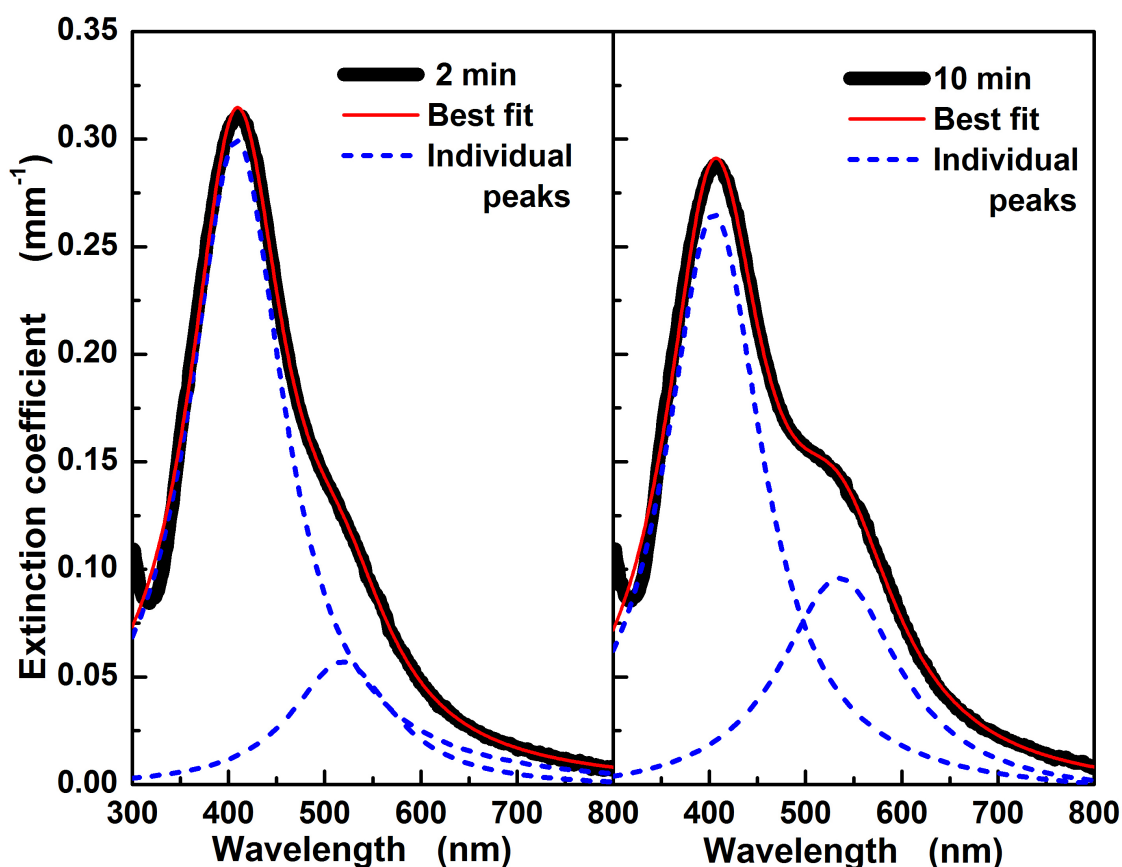


Figure 3: Extinction spectrum of the mixed sample (black lines) after (a) 2 min and (b) 10 min. Best fit to these experimental spectra using two Gaussian peaks (red lines). The contribution from individual peaks are also shown (blue lines).

A self-organized growth of Ag-CdTe hybrid nanostructure is expected in the mixed sample because of the tendency of TGA to get attached on the surface of Ag NP [27, 35, 36]. As the TGA is already attached to the CdTe QD, these QDs are also brought in close proximity to the Ag NP [27, 35, 36]. The final structure of hybrid formed by this self-organized growth process depends on the ratio between number of Ag NPs and CdTe QDs in the mixture, properties of the capping agents, size and shape of the individual particles. When Ag NP and CdTe QD colloids are mixed in a ratio of $\gamma = 0.56$, hybrid nanostructures of Ag NP surrounded by nearly 45 CdTe QDs ($H_{0.56}$ or Ag-nCdTe) are formed [27]. Once the CdTe QDs surrounds the Ag NP completely, it prevents further attachment of CdTe QD on to the Ag NP thus making the final hybrid structure stable. The extinction spectrum of the $H_{0.56}$ sample thus formed is also shown in Fig.2a for comparison. Clearly the extinction spectrum of this $H_{0.56}$ sample is very different from that of the H_{50} sample. The $H_{0.56}$ has an increasing absorption strength towards UV similar to that of bare CdTe QD colloid. On the other hand the H_{50} sample shows a dip in absorption around 320 nm which resembles more of Ag NP colloid. The AFM images of the H_{50} sample dried on mica shows several twin particles of each having nearly 17 nm height (Fig.2c). Based on the height, each of these particles should be the Ag NPs present in the mixed colloid.

The mixing ratio used for the sample H_{50} shows that there are nearly two Ag NPs for each CdTe QD. The number density of Ag NPs and CdTe QDs in the individual colloids were also estimated by using the numerically calculated extinction cross-section of a single Ag NP and CdTe QD and comparing it with the corresponding experimental extinction spectrum. The number densities estimated by using this procedure is also in agreement with the 2:1 number ratio of Ag NPs and CdTe QDs. Based on the number density estimation and the tendency of TGA to get attached to the Ag surface [35, 36],

we propose that in the final hybrid colloid, there are nanostructures with two Ag NPs attached to a single CdTe QD.

If a mixed hybrid sample was prepared with mixing ratio γ higher than 50, stable colloid do get formed. The final extinction spectrum of these hybrid colloids ($\gamma > 50$) has an extinction spectrum that looks similar to that observed in the intermediate stages (Fig.2b). For these γ values, there will not be enough CdTe QDs to join all the Ag NPs leaving several unattached Ag NPs along with few Ag\CdTe/Ag hybrids [27]. On the other hand, if the mixing ratio is lower than 50, aggregated nanostructures were found to settle down at the bottom of the sample. This can be explained by the presence of excess CdTe QDs which can link several Ag\CdTe/Ag NPs forming large chain-like structures which eventually becomes heavy enough to settle down [37, 38].

To understand the time evolution of the measured extinction spectra after mixing and to further understand the structure of the final hybrid formed, optical response of various Ag-CdTe hybrid nanostructures were numerically calculated using T-matrix technique (Fig.4). T-matrix is a numerical method for computing optical response of a collection of spherical particles [39, 40]. For Ag NPs of size of the order of 17 nm quantum confinement effects can be neglected and hence experimental bulk dielectric constants were used for the optical response calculations [41]. On the other hand, dielectric constant of a CdTe QD of size 3.5 nm will be substantially different from that of its bulk because of the quantum confinement effect [42]. The dielectric constant of CdTe QD was estimated using the method reported by Marcelo Alves-Santos *et al.* which uses the measured extinction spectrum and a trial and error procedure [42]. In the colloidal solution, it is expected that particles will be oriented in all possible directions. To mimic that situation with minimal computational cost, the extinction spectrum is estimated by averaging the responses calculated for a given field direction and particles

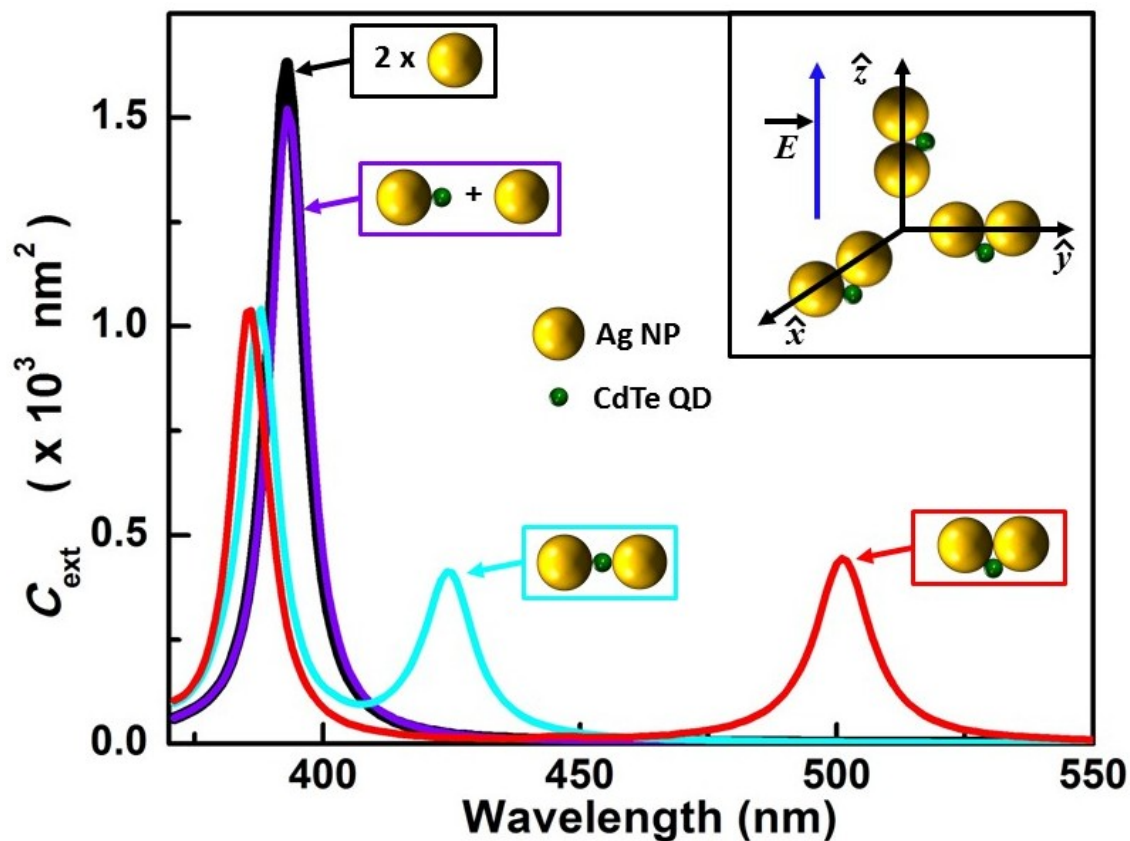


Figure 4: Calculated extinction cross-section of two non-interacting Ag NPs, attached Ag-CdTe particles, chain of Ag-CdTe-Ag particles and touching Ag-Ag particles with CdTe using T-matrix.

aligned along the three Cartesian directions (see inset of Fig.4) [40, 43].

The extinction cross-section of the Ag NP shows a single peak at 393 nm (Fig.4). In order to compare with the other structures where two Ag NPs are involved, C_{ext} of the two isolated Ag NPs (same as cross-section of single Ag NP multiplied by two) is plotted in the Fig.4. Once the Ag NP and the CdTe QD colloids were mixed, the most possible situation would be that a single CdTe QD will get attached to a single Ag NP. The second Ag NP would not have joined yet. To mimic such situation we have calculated C_{ext} of a single CdTe QD attached with an Ag NP and another Ag NP placed sufficiently away from it. The C_{ext} thus obtained shows a red-shift of about 1 nm when compared to that of isolated Ag NP. Further, the peak height also reduces to

about 90% of that of two isolated Ag NPs. Attaching a higher refractive index material to a metal nanoparticle is known to red-shift its LSPR peak [44, 45]. The changes in C_{ext} , the red-shift and the reduction in peak strength, when CdTe is attached to one of the Ag NP matches well with the observed change in the extinction spectrum measured nearly a minute after mixing Ag NP and CdTe QD colloids (Fig.2(b)). When another Ag NP is attached to the other end of CdTe QD which is already attached to an Ag NP, it will result in the formation of a linear Ag-CdTe-Ag structure. The C_{ext} of this structure shows a new peak at 424 nm and the original LSPR peak which was at 393 nm blue-shifts by 5 nm to 388 nm. These LSPR peaks, 424 nm and 388 nm appear when, field is aligned along the line joining the centers of the two Ag spheres (longitudinal axis) and perpendicular to it (transverse axis) respectively (Fig.4). Fitting the measured extinction spectrum at 2 min after mixing shows a double peak structure which matches well with that of C_{ext} of Ag-CdTe-Ag (Fig.3). The final spectrum of the hybrid has a second peak at 535 nm which is much more red-shifted compared to that calculated for the Ag-CdTe-Ag structure. Although capping prevents Ag NPs to join together, once brought in close proximity to each other, the metal particles do tend to join and restructure themselves [46–48]. Thus, once joined by the CdTe QD it is possible that over time the linear Ag-CdTe-Ag hybrid changes its structure to that with two Ag NPs touching each other with CdTe QD pushed to one side (Ag\CdTe/Ag) as shown in Fig.4. The calculated C_{ext} of Ag\CdTe/Ag hybrid match closer to the experimentally observed final extinction spectrum which has peaks at 408 nm and 535 nm (Fig.2a). Thus the peak at 408 nm corresponds to the LSPR originating when the field is aligned along the transverse axis (T-LSPR). Similarly the 535 nm peak corresponds to the LSPR when field is aligned along the longitudinal axis (L-LSPR).

Comparing the measured temporal evolution of the extinction spectra (Fig.2b) and

the calculated optical responses of the Ag NP and hybrid nanostructures (Fig.4), the growth of the final hybrid nanostructure can now be explained. Just after mixing, CdTe QD gets attached to Ag NP forming a large number of hybrid nanostructures each with one Ag NP and one CdTe QD. Such Ag-CdTe hybrid structure coexist in the colloidal solution along with almost equal number of unattached Ag NPs. This is indicated by the observed small red-shift and reduction in strength of the LSPR peak when measured 1 min after mixing (Fig.S2). As time progresses, another Ag NP also gets attached to the Ag-CdTe nanostructure to form an Ag-CdTe-Ag linear hybrid nanostructure. The observed second peak on the red-side of the extinction spectra measured in the first few minutes indicates the formation of such structures. Followed by this, the linear Ag-CdTe-Ag structure realign themselves to form Ag\CdTe/Ag structure. This explains the observed red-shifting of the long wavelength peak which finally settles down at 535 nm. To further confirm these observations we have also prepared Ag\CdTe/Ag hybrids with larger Ag NPs with diameter nearly 50 nm (Fig.S4). Once again the experimental results matches well with that of the calculated using T-matrix. Thus the final stable colloid, H₅₀ should have hybrid nanoparticles of Ag\CdTe/Ag structure. The size of the CdTe QD is much smaller and is now in between two large Ag NPs, further attachment of Ag NP to the same CdTe QD is prevented. Because of the limitation in resolution, the AFM image could not resolve the presence of small CdTe QD sitting in between the larger Ag NPs. Thus the AFM images of the Ag\CdTe/Ag hybrid show only a Ag NP dimer-like structure (Fig.2c). In some of the AFM images of H₅₀, we find few hybrid structures with Ag NPs attached to each other in triangular formation and few Ag NPs in chain-like structure (inset of Fig.S3). The T-matrix calculation shows that these triangular and chain-like structures have a very different extinction spectra compared to that observed in the experiment (Fig.S3). Transmission electron

microscope (TEM) could also be used for studying the structure of final self-aggregated Ag\Cdte/Ag nanostructures. Figure.5 shows some of the TEM images of the colloid containing Ag\Cdte/Ag hybrid nanostructures. The presence of the capping agents (polymers) in hybrid sample makes the process of capturing TEM images very difficult. Removal of these polymer by centrifuging would also destroy the hybrid nanostructure which is present in the colloidal solution. Further, during TEM studies, the measurement had to be performed at very low irradiation and the images had to be accrued quickly. Sometimes during the measurement, we still find that the particle do disappear during image accusation. The TEM images of Ag\Cdte/Ag hybrid nanostructures clearly shows presence of a smaller particle (size in the range of CdTe QDs) in between two larger sized particles (size of the order of Ag NPs) which matches well with that of expected from optical characterization (Fig.5).

It is interesting to note that the observed strengths of the LSPR peaks in te case of Ag\CdTe/Ag hybrid colloid can be explained by a simple model based on the orientation of the particles. Because of spherical symmetry, all the Ag NPs in the colloid absorbs the incident light irrespective of its polarization. Although in a colloidal sample all orientations of Ag\CdTe/Ag nanoparticle is possible, consider a simpler picture where all the particles are randomly aligned parallel to one of the three Cartesian directions with equal probability (inset of Fig.4). Such assumption in the distribution of particles has been shown to match well with that of the measured optical response of colloid containing randomly oriented ellipsoids and nanoprisms [37, 43]. Let the electric field be aligned to one of the Cartesian direction, about 66.7% ($2/3^{rd}$) of the particles will contribute to the T-LSPR peak (at 410 nm) because for these particles the polarization of light is oriented along the transverse axis. Whereas the rest 33.3% ($1/3^{rd}$) of the particles has their longitudinal axis aligned along the polarization and will show resonance at L-

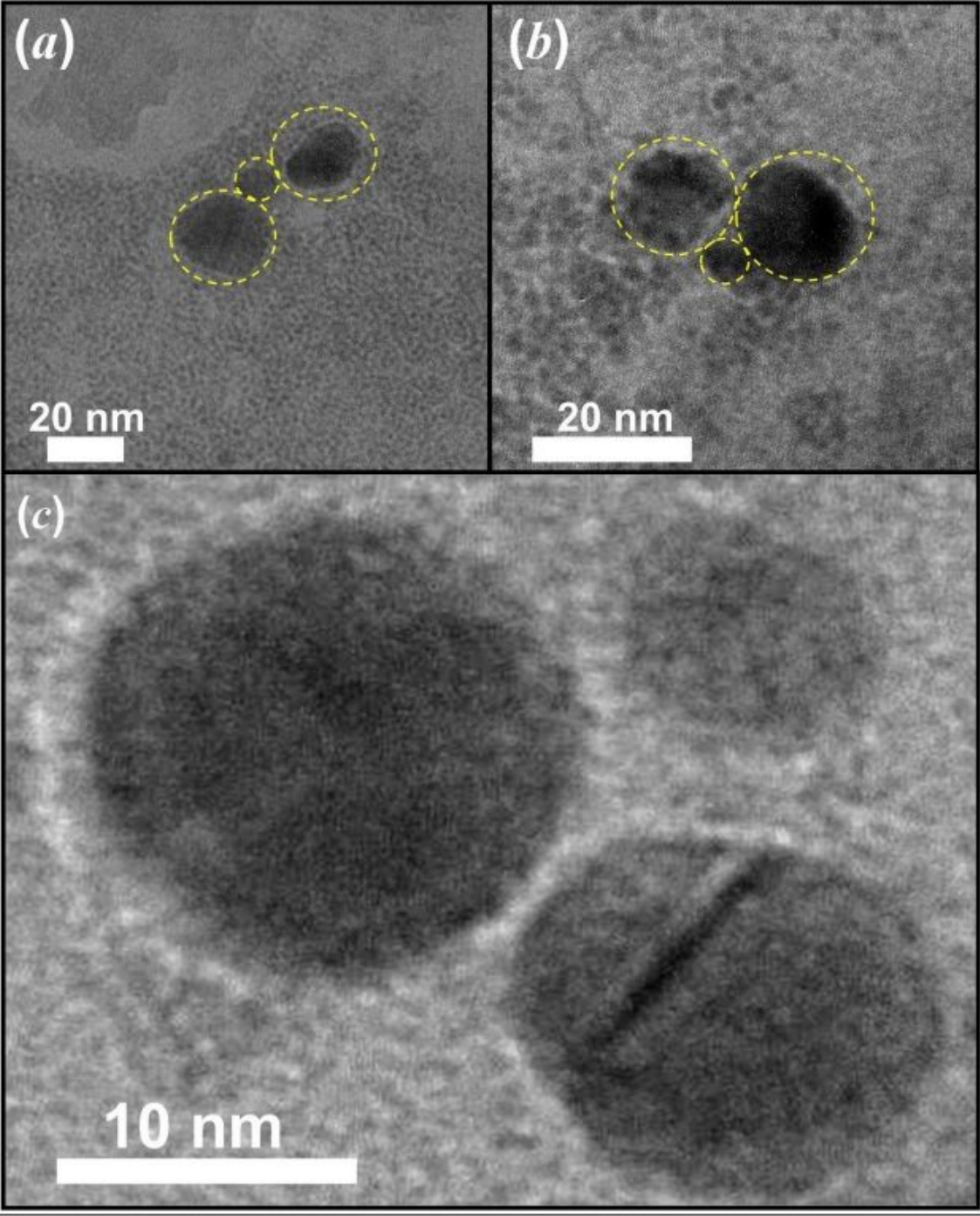


Figure 5: TEM images of Ag\Cdte/Ag hybrid nanostructures.

LSPR (535 nm). The measured LSPR peak heights for Ag\CdTe/Ag hybrid colloid at 410 nm and 535 nm are 65% and 32% of that of Ag NP colloid at its LSPR peak which are very close to that predicted by the model. This also implies that the C_{ext} of a Ag\CdTe/Ag particle is exactly same as that of two isolated Ag NPs if polarization is appropriately aligned. The reduction in C_{ext} of the Ag\CdTe/Ag hybrid colloid is mainly caused by the random orientations of the particles.

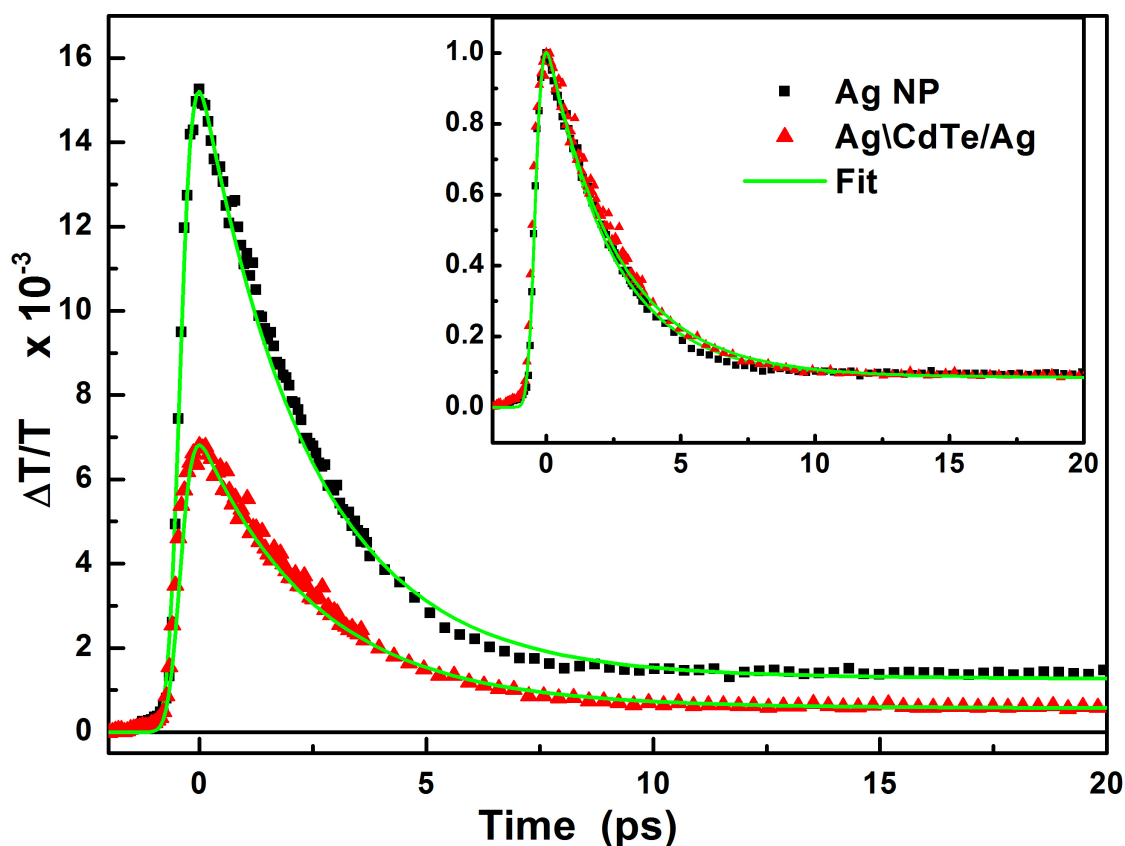


Figure 6: Transient curve of Ag NPs and Ag\CdTe/Ag hybrid colloidal samples excited at 400 nm and probe at 408 nm. Inset shows the normalized transient curve of these samples.

Figure.6 and Figure.7 shows the transient transmission signal ($\Delta T/T$) measured for the bare Ag NP and Ag\CdTe/Ag hybrid when probed at 408 nm and 550 nm respectively. In all these measurements the pump wavelength (400 nm) and pump fluence ($2.1 \mu\text{Jmm}^{-2}$) at the sample place were kept same. For both the samples and

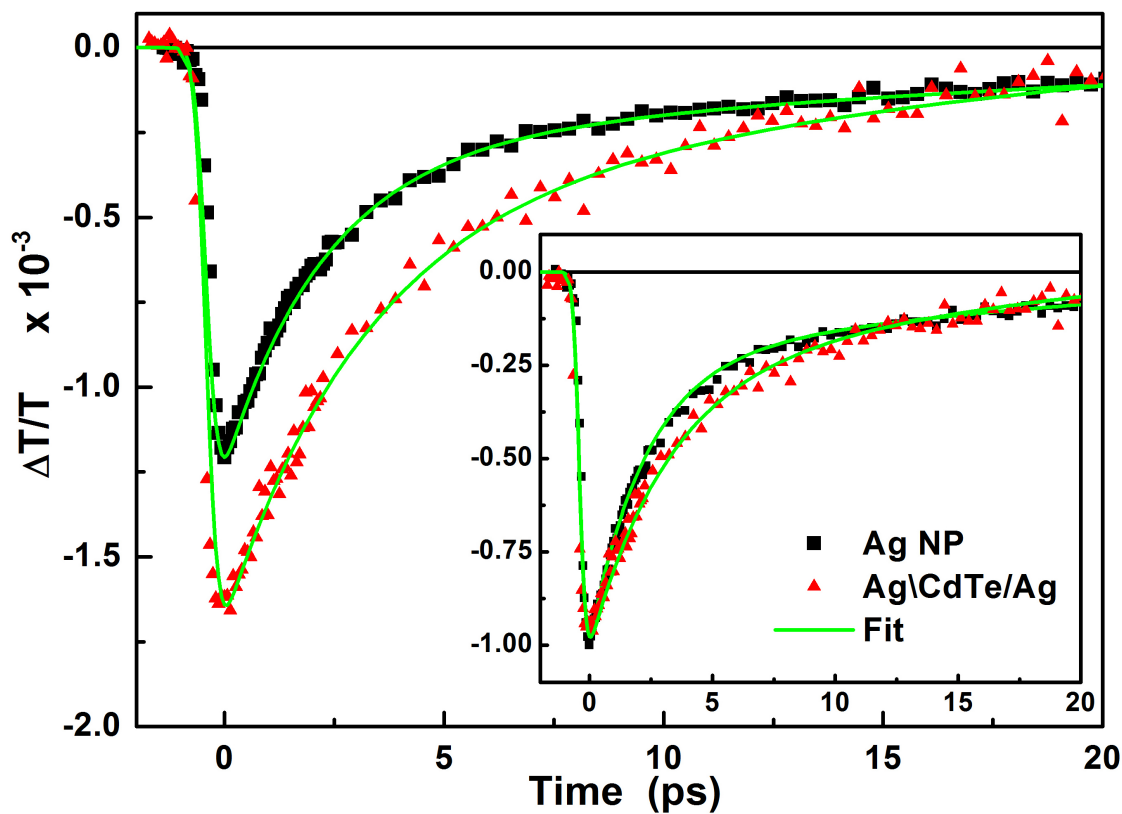


Figure 7: Transient transmission curve of Ag NPs and Ag\CdTe/Ag hybrid colloidal samples excited at 400 nm and probe at 550 nm. Inset shows the normalized transient curve of these samples.

at both probe wavelengths, the magnitude of $\Delta T/T$ ($|\Delta T/T|$) increases, reaching a maximum by about 400 fs. With further increase in the pump-probe delay, $|\Delta T/T|$ starts recovering, reaching a very low value by about 20 ps. Further, we find that sample containing bare CdTe QD colloid of concentration similar to that used in forming the Ag\CdTe/Ag hybrid colloid did not show any measurable $\Delta T/T$ signal.

The origin of ultrafast optical response of the bare metal NP colloid has been reported by several groups [49–53]. When a ultrashort pulse excites a metal nanoparticle at its LSPR, the free-electrons in the particles are set to oscillate in phase with the applied field. Within next few femtoseconds, these electrons decay to single-particle states through Landau-damping [49]. The energy distribution among electrons at this

stage will be non-thermal. These electrons relaxes to a thermalized high temperature state mainly through electron-electron scattering by about few hundreds of femtoseconds [51]. With increase in temperature of free-electrons, the real part of dielectric constant of Ag also increases which red-shifts the LSPR peaks [51–53]. This shift causes a change in the transmission of a metal NP colloid. The peak change in the transient transmission occur at the time when there is a maximum change in temperature of the free-electrons. In the present case of bare Ag NP colloid, when excited at 400 nm, the peak in $|\Delta T/T|$ occurs nearly after 400 fs irrespective of probe wavelength. Further, the red-shift of LSPR will cause an increase in transmission, when probed at 408 nm (blue-side of LSPR), and reduction in transmission when probed at 550 nm. Thus, the difference in probing wavelength with respect to LSPR causes the change in the sign of the measured $\Delta T/T$ in the case of Ag NP colloid (Fig.6 and Fig.7).

At the end of thermalization, the temperature of free-electrons is much higher whereas the lattice still remains almost at room temperature. Over a time of next few picoseconds, electron-phonon interaction leads to thermalization of electrons and lattice to a much lower temperature. This is due to the fact that the specific heat capacity of lattice is much higher than that of electrons. The thermalization process of electrons and lattice can be quantitatively understood using two-temperature model [51–53]. However, the two-temperature model would not be, in principle, directly applicable for hybrid nanostructures. In the present case, because hybrid nanostructures are also understudy, the complete temporal evolution of $\Delta T/T$ was fitted to,

$$F(t) = \frac{1}{2} [\mathcal{E}(t/t_r) + 1] \left[\sum_k A_k e^{-t/t_k} \right] \quad (1)$$

where $\mathcal{E}(x)$ is the Gauss error function of x , A_k and t_k are the amplitude and decay time respectively. The best fit to the experimental data using Eq.1 is also shown in Fig.6 and Fig.7. In the case of the bare Ag NP colloid, the best fit value of electron-phonon

thermalization time (τ_{ep}) probed at 408 nm and 550 nm are $2.3 \text{ ps} \pm 100 \text{ fs}$ and $2.4 \text{ ps} \pm 100 \text{ fs}$ respectively.

Similar to the bare Ag NP colloid, the sign of $\Delta T/T$ of Ag\CdTe/Ag hybrid colloid also changes from positive to negative when probe wavelength is changed from 408 nm to 550 nm. This shows that the transient response of Ag\CdTe/Ag is strongly similar to that of pure Ag NP colloid. To compare the temporal response, $\Delta T/T$ normalized to the peak change in $|\Delta T/T|$ ($|\Delta T/T|_{pk}$) are also shown in the inset of Fig.6 and Fig.7. The best fit to the decay times of $\Delta T/T$ for Ag\CdTe/Ag hybrid colloid when probed at 408 nm and 550 nm are $2.6 \text{ ps} \pm 100 \text{ fs}$ and $3.2 \text{ ps} \pm 100 \text{ fs}$ respectively. Clearly, when probed at 408 nm the recovery of change in transmission of the Ag\CdTe/Ag hybrid colloid is slightly slower than Ag NP colloid whereas at 550 nm it takes much longer to recover.

Electron-phonon relaxation takes a longer time in a single crystal Ag NP compared to that of crystal having twin defects because of the additional scattering of electrons at the lattice defects [15]. In the present case, the lattice quality of the bare Ag NPs and Ag\CdTe/Ag hybrid colloids should be same because the later is derived from the former. Further, the simple linking of Ag NPs by the CdTe QD should not change its crystal quality. Thus the increase in the relaxation time for the Ag\CdTe/Ag hybrid colloid cannot be explained by an improvement in lattice quality. At low temperatures, the electron-phonon relaxation time also depends on its temperature itself, increasing linearly with it [50]. Thus if the increase in the temperature of Ag in the Ag\CdTe/Ag hybrid nanostructure is more, then it can also show an increased electron-phonon relaxation time. The comparison between the measured $|\Delta T/T|_{pk}$ for different samples will be able to give some information about the maximum temperature reached by the free-electrons in the Ag NPs.

If $\Delta\varepsilon'_m$ is the small change in real part of dielectric constant due to the change in electron temperature, then the change in transmission at the probe wavelength ($\Delta T/T$) of a colloid having randomly oriented ellipsoidal particle can be written as [50, 53],

$$\frac{\Delta T}{T} = \frac{2\pi p}{3\lambda_{pr}\sqrt{\varepsilon_s}} \sum_{j=x,y,z} \text{Im} [f_j^2(\lambda_{pr})] \Delta\varepsilon'_m(\lambda_{pp}, \lambda_{pr}). \quad (2)$$

where p is the volume fraction, ε_s is the dielectric constant of the surrounding medium, f_j is the local field factor for j^{th} principle axis [1]. Because the change in dielectric constant is induced by the pump pulse and is sensed at probe wavelength, $\Delta\varepsilon'_m$ should depend on both the pump and probe wavelengths and their polarizations with respect to the orientation of the particle. For sufficiently small absorbed pump energies, $\Delta\varepsilon'_m$ depends linearly on absorbed power per unit volume of the particle [53]. For small particles, the contribution to the extinction cross-section is mainly dominated by absorption. Thus, $\Delta\varepsilon'_m$ is expected to be directly proportional to the extinction cross-section of the particle.

The $|\Delta T/T|_{pk}$ of Ag NP colloid when probed at 550 nm is much lower (only 9%) than that when probed at 408 nm. When pumped at 400 nm, irrespective of the polarization, all the Ag NPs absorbs the light. The change in the temperature of free-electrons will be proportional to the C_{ext} of a single Ag NP. When probed at 408 nm, all the Ag NPs will contribute to the $|\Delta T/T|_{pk}$ and the contribution from $\text{Im} [f_j^2]$ is also strong near to the LSPR (Fig.8 a). However, when probed at 550 nm which is far separated from LSPR, the contribution to $|\Delta T/T|_{pk}$ from $\text{Im} [f_j^2]$ reduces considerably [53–55], reducing the measured $|\Delta T/T|_{pk}$. Because the pump fluence is same in both of these case the decay time will also remain same irrespective of the probe wavelength.

Consider the simple model of Ag\CdTe/Ag particles oriented along the three Cartesian directions. In Fig.8, schematic of particles oriented in three different directions along with the polarizations of the pump and probe beams used in the experiments are

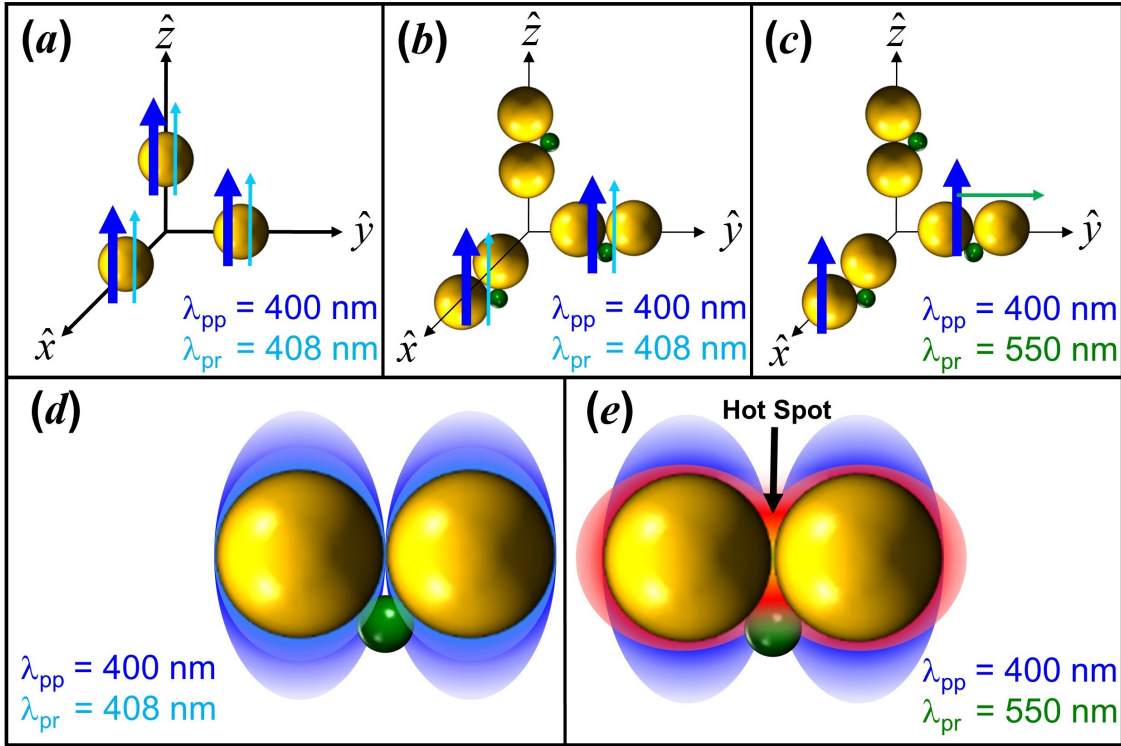


Figure 8: Schematic of particles oriented in three different directions along with polarization of pump and probe pulse. Blue thick line indicates polarization of pump pulse(400 nm) and thin line, blue(408 nm) and green(550 nm), indicates polarization of probe pulse.

shown. As discussed in the case of static optical response, when the particle is aligned along the transverse axis, its C_{ext} will remain nearly same as that of two isolated Ag NPs. Thus when excited at 400 nm, close to T-LSPR, nearly $2/3^{rd}$ of the Ag\CdTe/Ag hybrid particles will absorb the light and the increase in temperature of free-electrons will also be nearly same as that of the isolated Ag NP for the same pump fluence. When probed at 408 nm, the factor $Im[f_j^2]$ will also be finite and all the excited Ag\CdTe/Ag particles (which is only $2/3^{rd}$ of the total) will contribute to $|\Delta T/T|_{pk}$. Thus the $|\Delta T/T|_{pk}$ measured for Ag\CdTe/Ag hybrid colloid should be lesser by at least a factor of $2/3^{rd}$ compared to that of Ag NP colloid probed at 408 nm. With a similar argument it can be shown that the $|\Delta T/T|_{pk}$ of Ag\CdTe/Ag hybrid colloid probed at 550 nm, close to L-LSPR, should be lesser by at least a factor of $1/3^{rd}$ compared to that of Ag NP colloid

probed at 408 nm (Fig.8c). The $|\Delta T/T|_{pk}$ measured for the Ag\CdTe/Ag hybrid colloid is about $\sim 44\%$ and 11% when probed at 408 nm and 550 nm respectively, compared to that of Ag NP colloid at 408 nm. Thus, the measured $|\Delta T/T|_{pk}$ of Ag\CdTe/Ag hybrid colloid at these wavelengths were even lower than that estimated. Based on this observation, the increase in temperature of free-electrons in the Ag NPs of Ag\CdTe/Ag hybrids should be same or lower than that of the particles in bare Ag NP colloid. Thus the electron-phonon relaxation time measured for Ag\CdTe/Ag hybrid colloid should have remained same or reduced than that of Ag NP colloid, which is opposite to that of observed in the experiment. Hence, change in the absorbed power cannot explain the increase in the relaxation time measured for Ag\CdTe/Ag hybrid colloid.

Prashant K. Jain *et al.* studied the transient change in the optical response of aggregated gold nanoparticles when excited at 400 nm [56]. Their result show that the electron-phonon relaxation time is smaller when probed at the longer-wavelength LSPR peak compared to that measured at the shorter wavelength. They have attributed this reduction to the increased overlap of the longer wavelength LSPR with the phonon spectrum and also to the enhanced interfacial electron scattering [56]. Similar reduction in electron-phonon relaxation time has also been reported for other Au and Ag nanoparticle aggregates [57,58]. This implies that the interaction between two metal nanoparticles should lead to a reduction in the relaxation time of the $\Delta T/T$, which is again opposite of what is observed in the present case. Thus, presence of CdTe QD in between the Ag nanoparticles is indeed playing a role in the dynamics observed in Ag\CdTe/Ag colloid.

When a metal nanoparticle is attached to a semiconductor, three different processes starts modifying the response of the combined super-structure. A direct metal-to-semiconductor interfacial charge transfer, which occurs through direct excitation of

electron from metal NPs to empty states in semiconductor [59–61]. Such transfer is more possible in hybrid systems where semiconductor is in direct contact with the surface of the metal. In some hybrid cases, the metal NP absorbs the light creating hot-electrons, which then gets transferred to the empty levels in semiconductor. Signature of such hot-electron transfer from metal NP to semiconductor QD has been observed in several hybrid nanostructures [59, 60, 62]. Even if there is no direct contact between the metal and semiconductor, hot-carrier transport still occurs via the linking polymer/molecule [30, 50]. In addition to the above mentioned processes, a direct energy transfer between metal and semiconductor is also possible, if the LSPR of metal nanoparticle overlaps with the absorption spectrum of semiconductor QD [63, 64].

Charge or energy transfer between the constituents of a hybrid strongly depends on the final superstructure formed by the metal-semiconductor nanostructures [30, 50, 65]. When the Ag\CdTe/Ag hybrid colloid is pumped at 400 nm, T-LSPR is excited in the Ag NPs and at the same time it can also excite carriers in CdTe from valance band to conduction band. A comparison of temporal response of $\Delta T/T$ of Ag NP colloid and Ag\CdTe/Ag colloid when probed at 408 nm shows that the dynamics in this system is dominated by the plasmonic response of a Ag NP. Even if carriers are excited in CdTe QDs, when probed well above the band edge, CdTe QDs do not show significant change in its transient response [30]. Further, exciting at 400 nm, resonant to T-LSPR, does not create "hot-spot" in between the Ag NPs where CdTe QD is located (Fig.8d). Thus probing the Ag\CdTe/Ag colloid at 408 nm strongly resembles the dynamics of Ag NP colloid (Fig.6). On the other hand, when probed at 550 nm, the probe pulse can sense the presence of CdTe QD because probe field gets enhanced at the location of CdTe QD. Further, CdTe QD can also show a strong transient change in transmission when probed at 550 nm. Thus, although a significant contribution of metallic response is expected

near to the L-LSPR, the Ag\CdTe/Ag hybrid colloid, when probed at 550 nm show a longer response time than that of bare Ag NP colloid.

4. Conclusion

When Ag NP colloid is mixed with TGA capped CdTe QD colloid such that in the mixed colloid the number ratio between the Ag NPs and CdTe QDs is 2:1, stable hybrid nanostructure with two Ag NPs and a CdTe could be formed. Optical spectra during growth and transient optical response suggests that the final structure has two touching Ag nanoparticle with CdTe QD stuck in between them. The static optical response of the final hybrid colloid could be explained well by the electromagnetic interaction between these particles present in the structure. Assuming that the extinction cross-section of each Ag NP in the Ag\CdTe/Ag hybrid structure to be same as that of an isolated Ag NP, the optical response of Ag\CdTe/Ag colloid could be explained by their random orientations in the host. When excited and probed near the T-LSPR, the ultrafast optical response of Ag\CdTe/Ag hybrid nanostructure resembles that of a bare Ag NP. On the other hand while probing at the L-LSPR show a delayed recovery of transient transmission. This is attributed to the sensing of presence of CdTe QD in the hot-spot regime by the probe field. Placing a semiconductor QD at or close to the hot-spot is a major step towards using the enhanced local field in various applications such as plasmonic sensing, optoelectronics, energy harvesting, nanolithography, and optical nano-antennas. Further, these studies are also important for the advancement in the area of colloidal self-assembly, with impacts on the dynamic properties of hot spots for specific needs [66,67].

Acknowledgments

The authors are thankful to Tarun Kumar Sharma, Rama Chari and Salahuddin Khan for fruitful discussions and suggestions. The authors are also thankful to Arvind Kumar Srivastava for the support in obtaining the TEM images. The authors, Sabina Gurung and Durga Prasad Khatua are thankful to RRCAT, Indore, under HBNI programme, Mumbai, for the financial support.

References

- [1] Craig F Bohren and Donald R Huffman. *Absorption and scattering of light by small particles*. John Wiley & Sons, 2008.
- [2] Palash Bharadwaj, Pascal Anger, and Lukas Novotny. Nanoplasmonic enhancement of single-molecule fluorescence. *Nanotechnology*, 18(4):044017, 2006.
- [3] M Futamata, Y Maruyama, and M Ishikawa. Local electric field and scattering cross section of Ag nanoparticles under surface plasmon resonance by finite difference time domain method. *J. Phys. Chem. B*, 107(31):7607–7617, 2003.
- [4] KR Catchpole, , and Albert Polman. Plasmonic solar cells. *Opt. Express*, 16(26):21793–21800, 2008.
- [5] Julia A Ruennele, W Paige Hall, Laura K Ruvuna, and Richard P Van Duyne. A localized surface plasmon resonance imaging instrument for multiplexed biosensing. *Anal. Chem.*, 85(9):4560–4566, 2013.
- [6] Harry A Atwater and Albert Polman. Plasmonics for improved photovoltaic devices. In *Materials For Sustainable Energy: A Collection of Peer-Reviewed Research and Review Articles from Nature Publishing Group*, pages 1–11. World Scientific, 2011.
- [7] Scott K Cushing and Nianqiang Wu. Plasmon-enhanced solar energy harvesting. *Electrochem. Soc. Interface*, 22(2):63–67, 2013.
- [8] Ruibin Jiang, Benxia Li, Caihong Fang, and Jianfang Wang. Metal/semiconductor hybrid nanostructures for plasmon-enhanced applications. *Adv. Mater.*, 26(31):5274–5309, 2014.
- [9] Wenguang Fan and Michael KH Leung. Recent development of plasmonic resonance-based photocatalysis and photovoltaics for solar utilization. *Molecules*, 21(2):180, 2016.

- [10] Yinghui Sun, Xianzhong Yang, Haofei Zhao, and Rongming Wang. Non-symmetric hybrids of noble metal-semiconductor: Interplay of nanoparticles and nanostructures in formation dynamics and plasmonic applications. *Prog. Mater. Sci.: Materials International*, 27(2):157–168, 2017.
- [11] Heesang Ahn, Hyerin Song, Jong-ryul Choi, and Kyujung Kim. A localized surface plasmon resonance sensor using double-metal-complex nanostructures and a review of recent approaches. *Sensors*, 18(1):98, 2018.
- [12] Wen Xu, Yongsheng Zhu, Xu Chen, Jing Wang, Li Tao, Sai Xu, Tong Liu, and Hongwei Song. A novel strategy for improving upconversion luminescence of $\text{NaYF}_4:\text{Yb, Er}$ nanocrystals by coupling with hybrids of silver plasmon nanostructures and poly(methyl methacrylate) photonic crystals. *Nano Research*, 6(11):795–807, Nov 2013.
- [13] Encai Hao and George C Schatz. Electromagnetic fields around silver nanoparticles and dimers. *J. Chem. Phys.*, 120(1):357–366, 2004.
- [14] Eleonora Petryayeva and Ulrich J Krull. Localized surface plasmon resonance: Nanostructures, bioassays and biosensing—a review. *Anal. Chim. Acta*, 706(1):8–24, 2011.
- [15] Yun Tang and Min Ouyang. Tailoring properties and functionalities of metal nanoparticles through crystallinity engineering. *Nat. Mater.*, 6(10):754, 2007.
- [16] Pedro HC Camargo, Leslie Au, Matthew Rycenga, Weiyang Li, and Younan Xia. Measuring the SERS enhancement factors of dimers with different structures constructed from silver nanocubes. *Chem. Phys. Lett.*, 484(4-6):304–308, 2010.
- [17] Yi Luo and Jing Zhao. Plasmon-exciton interaction in colloiddally fabricated metal nanoparticle-quantum emitter nanostructures. *Nano Research*, 12(9):2164–2171, Sep 2019.
- [18] Yuhua Feng, Jiating He, Hong Wang, Yee Yan Tay, Hang Sun, Liangfang Zhu, and Hongyu Chen. An unconventional role of ligand in continuously tuning of metal–metal interfacial strain (*J. Am. Chem. Soc.*, 2012).
- [19] Paul R. Mark. *Forces and interactions between nanoparticles for controlled structures*. PhD thesis, Graduate School-New Brunswick Rutgers, The State University of New Jersey, 2013.
- [20] Weiyang Li, Pedro HC Camargo, Xianmao Lu, and Younan Xia. Dimers of silver nanospheres: facile synthesis and their use as hot spots for surface-enhanced raman scattering. *Nano Lett.*, 9(1):485–490, 2008.
- [21] Jonathan A. Fan, Chihhui Wu, Kui Bao, Jiming Bao, Rizia Bardhan, Naomi J. Halas,

- Vinothan N. Manoharan, Peter Nordlander, Gennady Shvets, and Federico Capasso. Self-assembled plasmonic nanoparticle clusters. *Science*, 328:1135–1138, 2010.
- [22] Eyal Cohen-Hoshen, Garnett W Bryant, Iddo Pinkas, Joseph Sperling, and Israel Bar-Joseph. Exciton–plasmon interactions in quantum dot–gold nanoparticle structures. *Nano Lett.*, 12(8):4260–4264, 2012.
- [23] Alejandro Manjavacas, Francisco Javier Garcia de Abajo, and Peter Nordlander. Quantum plexcitonics: strongly interacting plasmons and excitons. *Nano Lett.*, 11(6):2318–2323, 2011.
- [24] Rongchao Jin, YunWei Cao, Chad A Mirkin, KL Kelly, George C Schatz, and JG Zheng. Photoinduced conversion of silver nanospheres to nanoprisms. *Science*, 294(5548):1901–1903, 2001.
- [25] Jia Guo, Wuli Yang, and Changchun Wang. Systematic study of the photoluminescence dependence of thiol-capped CdTe nanocrystals on the reaction conditions. *J. Phys. Chem. B*, 109(37):17467–17473, 2005.
- [26] Abhijit Mandal and Naoto Tamai. Influence of acid on luminescence properties of thioglycolic acid-capped CdTe quantum dots. *J. Phys. Chem. C*, 112(22):8244–8250, 2008.
- [27] Sabina Gurung, Asha Singh, Rama Chari, and J Jayabalan. The optical response of self-organized Ag–CdTe metal–semiconductor hybrid nanostructures: Change in interaction vs number density variation. *J. Appl. Phys.*, 124(20):204305, 2018.
- [28] Christian Strelow, T Sverre Theuerholz, Christian Schmidtke, Marten Richter, Jan-Philip Merkl, Hauke Kloust, Ziliang Ye, Horst Weller, Tony F Heinz, Andreas Knorr, et al. Metal–Semiconductor nanoparticle hybrids formed by self-organization: A platform to address exciton–plasmon coupling. *Nano Lett.*, 16(8):4811–4818, 2016.
- [29] Yanfei Wang, Minjie Li, Huiying Jia, Wei Song, Xiaoxia Han, Junhu Zhang, Bai Yang, Weiqing Xu, and Bing Zhao. Optical properties of Ag/CdTe nanocomposite self-organized by electrostatic interaction. *Spectrochim. Acta, Part A*, 64(1):101–105, 2006.
- [30] Navendu Mondal and Anunay Samanta. Ultrafast charge transfer and trapping dynamics in a colloidal mixture of similarly charged CdTe quantum dots and silver nanoparticles. *J. Phys. Chem. C*, 120(1):650–658, 2015.
- [31] David Paramelle, Anton Sadovoy, Sergey Gorelik, Paul Free, Jonathan Hobley, and David G Fernig. A rapid method to estimate the concentration of citrate capped silver nanoparticles from UV-visible light spectra. *Analyst*, 139(19):4855–4861, 2014.

- [32] Sander F Wuister, Floris Van Driel, and Andries Meijerink. Luminescence of CdTe nanocrystals. *J. Lumin.*, 102:327–332, 2003.
- [33] W William Yu, Lianhua Qu, Wenzhuo Guo, and Xiaogang Peng. Experimental determination of the extinction coefficient of CdTe, CdSe, and CdS nanocrystals. *Chem. Mater.*, 15(14):2854–2860, 2003.
- [34] Wei Chen, Alan G Joly, and David E McCready. Upconversion luminescence from CdSe nanoparticles. *J. Chem. Phys.*, 122(22):224708, 2005.
- [35] Jin Chang, Yuhei Ogomi, Chao Ding, Yao Hong Zhang, Taro Toyoda, Shuzi Hayase, Kenji Katayama, and Qing Shen. Ligand-dependent exciton dynamics and photovoltaic properties of PbS quantum dot heterojunction solar cells. *Phys. Chem. Chem. Phys.*, 19(9):6358–6367, 2017.
- [36] Shane A Gallagher, Steve Comby, Michal Wojdyla, Thorfinnur Gunnlaugsson, John M Kelly, Yurii K Gun'ko, Ian P Clark, Gregory M Greetham, Michael Towrie, and Susan J Quinn. Efficient quenching of TGA-capped CdTe quantum dot emission by a surface-coordinated europium (III) cyclen complex. *Inorg. Chem.*, 52(8):4133–4135, 2013.
- [37] J Jayabalan, Asha Singh, Rama Chari, Himanshu Srivastava, PK Mukhopadhyay, AK Srivastava, and SM Oak. Aggregated nanoplatelets: optical properties and optically induced deaggregation. *J. Phys. Condens. Matter*, 20(44):445222, 2008.
- [38] Hafiz HM Salih, Amro M El Badawy, Thabet M Tolaymat, and Craig L Patterson. Removal of stabilized silver nanoparticles from surface water by conventional treatment processes. *Advances in Nanoparticles*, 8:21–35, 2019.
- [39] MI Mishchenko. Light scattering by randomly oriented axially symmetric particles. *J. Opt. Soc. Am. A*, 8(6):871–882, 1991.
- [40] Daniel W Mackowski and Michael I Mishchenko. Calculation of the T matrix and the scattering matrix for ensembles of spheres. *J. Opt. Soc. Am. A*, 13(11):2266–2278, 1996.
- [41] Peter B Johnson and R-W Christy. Optical constants of the noble metals. *Phys. Rev. B*, 6(12):4370, 1972.
- [42] Marcelo Alves-Santos, Rosa Di Felice, and Guido Goldoni. Dielectric functions of semiconductor nanoparticles from the optical absorption spectrum: the case of CdSe and CdS. *J. Phys. Chem. C*, 114(9):3776–3780, 2010.
- [43] K Lance Kelly, Eduardo Coronado, Lin Lin Zhao, and George C Schatz. The optical properties

- of metal nanoparticles: the influence of size, shape, and dielectric environment. *J. Phys. Chem. B*, 107:668–677, 2003.
- [44] L Genzel, TP Martin, and U Kreibig. Dielectric function and plasma resonances of small metal particles. *Z. Phys. B: Condens. Matter*, 21(4):339–346, 1975.
- [45] Jack J Mock, David R Smith, and Sheldon Schultz. Local refractive index dependence of plasmon resonance spectra from individual nanoparticles. *Nano Lett.*, 3(4):485–491, 2003.
- [46] Kevin G Stamplecoskie and Juan C Scaiano. Kinetics of the formation of silver dimers: early stages in the formation of silver nanoparticles. *J. Am. Chem. Soc.*, 133(11):3913–3920, 2011.
- [47] Michael Grouchko, Alexander Kamyshny, Cristina Florentina Mihailescu, Dan Florin Anghel, and Shlomo Magdassi. Conductive inks with a “built-in” mechanism that enables sintering at room temperature. *ACS Nano*, 5(4):3354–3359, 2011.
- [48] Michael Grouchko, Polina Roitman, Xi Zhu, Inna Popov, Alexander Kamyshny, Haibin Su, and Shlomo Magdassi. Merging of metal nanoparticles driven by selective wettability of silver nanostructures. *Nat. Commun.*, 5:2994, 2014.
- [49] Cyril Guillon, Pierre Langot, Natalia Del Fatti, and Fabrice Vallee. Ultrafast surface plasmon resonance Landau damping and electron kinetics in metal nanoparticles. *Ultrafast Phenomena in Semiconductors and Nanostructure Materials VIII*, 5352:65–76, 2004.
- [50] Asha Singh, Sabina Gurung, Rama Chari, and Jesumony Jayabalan. Counting the electrons hopping in ultrafast time scales in an Ag-CdTe hybrid nanostructure. *J. Phys. Chem. C*, 123:28584–28592, 2019.
- [51] N Del Fatti, C Voisin, M Achermann, S Tzortzakis, D Christofilos, and F Vallée. Nonequilibrium electron dynamics in noble metals. *Phys. Rev. B*, 61(24):16956, 2000.
- [52] J-Y Bigot, V Halté, J-C Merle, and A Daunois. Electron dynamics in metallic nanoparticles. *Chem. Phys.*, 251(1-3):181–203, 2000.
- [53] J Jayabalan. Origin and time dependence of higher-order nonlinearities in metal nanocomposites. *J. Opt. Soc. Am. B*, 28(10):2448–2455, 2011.
- [54] M Perner, S Gresillon, J März, G Von Plessen, J Feldmann, J Porstendorfer, K-J Berg, and G Berg. Observation of hot-electron pressure in the vibration dynamics of metal nanoparticles. *Phys. Rev. Lett.*, 85(4):792, 2000.
- [55] Rodrigo Sato, Masato Ohnuma, Keiji Oyoshi, and Yoshihiko Takeda. Experimental investigation of nonlinear optical properties of Ag nanoparticles: Effects of size quantization. *Phys. Rev. B*,

- 90(12):125417, 2014.
- [56] Prashant K Jain, Wei Qian, and Mostafa A El-Sayed. Ultrafast electron relaxation dynamics in coupled metal nanoparticles in aggregates. *J. Phys. Chem. B*, 110(1):136–142, 2006.
- [57] Mark J Feldstein, Christine D Keating, Yish-Hann Liao, Michael J Natan, and Norbert F Scherer. Electronic relaxation dynamics in coupled metal nanoparticles. *J. Am. Chem. Soc.*, 119(28):6638–6647, 1997.
- [58] Xiu-Chun Yang, Zhi-Wei Dong, Hui-Xin Liu, Jing-Xian Xu, and Shi-Xiong Qian. Effects of thermal treatment on the third-order optical nonlinearity and ultrafast dynamics of Ag nanoparticles embedded in silicate glasses. *Chem. Phys. Lett.*, 475(4-6):256–259, 2009.
- [59] Kaifeng Wu, Jinqun Chen, James R McBride, and Tianquan Lian. Efficient hot-electron transfer by a plasmon-induced interfacial charge-transfer transition. *Science*, 349(6248):632–635, 2015.
- [60] Akihiro Furube and Shuichi Hashimoto. Insight into plasmonic hot-electron transfer and plasmon molecular drive: new dimensions in energy conversion and nanofabrication. *NPG Asia Materials*, 9(12):e454, 2017.
- [61] Bo Gao, Yue Lin, Sijie Wei, Jie Zeng, Yuan Liao, Liuguo Chen, David Goldfeld, Xiaoping Wang, Yi Luo, Zhenchao Dong, and Jianguo Hou. Charge transfer and retention in directly coupled au-cdse nanohybrids. *Nano Research*, 5(2):88–98, Feb 2012.
- [62] Yuxin Tang, Zhelong Jiang, Guichuan Xing, Anran Li, Pushkar D Kanhere, Yanyan Zhang, Tze Chien Sum, Shuzhou Li, Xiaodong Chen, Zhili Dong, et al. Efficient Ag@ AgCl cubic cage photocatalysts profit from ultrafast plasmon-induced electron transfer processes. *Adv. Funct. Mater.*, 23(23):2932–2940, 2013.
- [63] Jamuna K Vaishnav and Tushar Kanti Mukherjee. Long-range resonance coupling-induced surface energy transfer from CdTe quantum dot to plasmonic nanoparticle. *J. Phys. Chem. C*, 122(49):28324–28336, 2018.
- [64] AE Ragab, A-S Gadallah, MB Mohamed, and IM Azzouz. Photoluminescence and upconversion on Ag/CdTe quantum dots. *Optics & Laser Technology*, 63:8–12, 2014.
- [65] Zhenfeng Bian, Takashi Tachikawa, Peng Zhang, Mamoru Fujitsuka, and Tetsuro Majima. Au/TiO₂ superstructure-based plasmonic photocatalysts exhibiting efficient charge separation and unprecedented activity. *J. Am. Chem. Soc.*, 136(1):458–465, 2013.
- [66] Darya Radziuk and Helmuth Moehwald. Prospects for plasmonic hot spots in single molecule SERS towards the chemical imaging of live cells. *Phys. Chem. Chem. Phys.*, 17(33):21072–

21093, 2015.

- [67] Eva-Maria Roller, Lucas V Besteiro, Claudia Pupp, Larousse Khosravi Khorashad, Alexander O Govorov, and Tim Liedl. Hotspot-mediated non-dissipative and ultrafast plasmon passage. *Nat. Phys.*, 13(8):761, 2017.